Vermessung & Geoinformation 2+3/2015, P. 188 – 197, 8 Figs.


Knot estimation on B-Spline curves

Claudius Schmitt and Hans Neuner, Wien

Abstract

Freeform curves with their possibility to approximate shapes from terrestrial laser scanner point clouds are investigated in this study. We focus on B-spline curves which are able to capture the local behavior of the measured profile. Typically, the only parameter set, treated as unknowns are the control points of the B-Spline. Their location is determined by least squares adjustment. The second parameter set are the knots, usually placed at stable locations and they are part of the basis functions. The approach with fixed number of knots placed at stable locations leads to a linear system. However, it intuitively restricts the B-Spline curve in its flexibility. Hence the residuals of the approximation may still contain systematic effects. Estimating the control points and the locations of the knots at the same time succeeds in full flexibility of B-Splines and optimizes the approximation. The system of equations accrued in this second case is highly non-linear. Adequate initial values are necessary to solve this system. Furthermore, introducing constraints can enhance the convergent behavior. This paper introduces a new method that allows the estimation of the number of knots as well as their location. The method uses a bottom up approach starting with the minimum number of knots, denoted as Bézier curves, and adding one knot in each iteration step at a particular curve sections (span) until the convergent criterion is reached. The decision to insert a knot and at a specific location, is based on the analysis of the cumulated sums of squared residuals in each existing span. The location, where the additional knot was inserted, is optimized using a Gauß-Markov model with constraints. The improvements are shown by comparing the results obtained in the linear approach with fixed knots and the non-linear case where control points and the knots are treated as unknowns.

Keywords: B-Spline curve, free knots, shape modelling, freeform curve, TLS profile approximation

Kurzfassung

Freiformkurven können zur Approximation von Punktwolken von terrestrischen Laserscannern genutzt werden. Im Speziellen werden in dieser Untersuchung B-Spline Kurven eingesetzt, die je nach Parameterwahl lokale Gegebenheiten in einer globalen Approximation darstellen können. Typischerweise werden bei einer Approximation von B-Splines die Kontrollpunkte in einem linearen Modell geschätzt. Die Knoten sind ein weiterer Parametersatz mithilfe derer die Basisfunktionen erstellt werden. Die gemeinsame Schätzung der Knoten mit den Kontrollpunkten ergibt ein hochgradig nichtlineares Gleichungssystem. Die volle Flexibilität zur lokalen Anpassung wird erst durch die Schätzung beider Parametergruppen erreicht. Zur Stützung des nichtlinearen Gleichungssystems werden Bedingungsgleichungen und verbesserte Näherungswerte eingeführt. Diese Näherungswerte für die Knoten werden mit einer neuen Methode ermittelt. Diese basiert auf den Residuen der linearen Schätzung der Kontrollpunkte, die in Teilbereichen, sogenannter Spans, analysiert werden. Begonnen wird die Approximation mit der Minimalkonfiguration, den Bézier-Kurven, innerhalb derer die Knoten festgelegt sind. Die im neuen Ansatz erzielte Verbesserung wird durch den Vergleich der Ergebnisse aus der Schätzung der Knoten und der Kontrollpunkte demonstriert.

Schlüsselwörter: B-Spline Kurve, Knotenschätzung, Oberflächenmodellierung, Freiformkurve, TLS Profilapproximation

1. Introduction

Surface-based metrology, like terrestrial laser scanning (TLS), needs new surface-based evaluation methods. Taking the workshop suggestions from [1] into account, these evaluation methods are one of the main challenges making the information of 3D point clouds suitable for further processing steps and taking benefits from the redundancy. Freeform curves and surfaces are promising approximation methods to create parameterized curves and surfaces, like shape information for structural-mechanic analysis of built objects [2]. Whereby, the freeform curves are the basis for the freeform surfaces. Past research has shown that the freeform shapes significantly improve the approximation quality, compared to approximations with geometric primitives, e. g. [2].

In this paper, B-Spline curves are used to approximate TLS profiles. In the past, only the control points of the B-Spline were estimated. Another essential parameter set for B-splines are the knots. The optimization of the knot-locations leads to a nonlinear system of equations. The solution of the non-linear problem as well as the determination of proper initial values for the knot positions is a challenge for which an innovative solution is presented in this paper.

The paper is structured as follows: aspects of B-Spline-curve theory are outlined in the 2nd chapter; the state of the art of curve approximation is presented in chapter 3. Chapter 4 introduces an example that motivates the necessity for knot estimation. The main concepts of the developed method for estimating the number of knots and their locations are described in chapter 5. Performance analysis and the validation of the method is done in chapter 6.1 for simulated data and in chapter 6.2 for real data.

2. B-Spline curves

For the spatial approximation of the TLS 2D profile, B-Spline curves are used. They were proposed by de Boor and de Casteljau [3], [4] and applied especially in CAD designs and construction of cars. The challenge in this paper is to use them in the opposite way, for approximating existing curves and surfaces, based on single points. The advantage of the B-Splines is their flexibility in matching most of the curves with respect to their local behavior.

The local behavior is due to the piecewise linear independent basis function, $N_{i,p}$, with its recursive definition:

$$N_{i,0}\left(obs_{Par.}\right)=\begin{cases}1 & if\ \ u_i < obs_{Par.} > u_{i+1}\\ 0 & otherwise\end{cases}, \quad (2.1)$$

$$N_{i,p}\left(obs_{Par.}\right)=\frac{obs_{Par.}-u_i}{u_{i+p}-u_i}N_{i,p-1}\left(obs_{Par.}\right)+ \\ +\frac{u_{i+p+1}-obs_{Par.}}{u_{i+p+1}-u_{i+1}}N_{i+1,p-1}\left(obs_{Par.}\right), \quad (2.2)$$

$$i = 0, \dots, n, \quad \text{with } U=\{u_0, \dots, u_m\} \text{ and} \quad (2.3)$$

$$m = n + p + 1, \quad (2.4)$$

where n is the number of basis functions and their corresponding control points. For further information on the recursive definition see [5]. The basis function, consists of divided differences of the knots u, with $m+1$ knots inside the knot vector U, and the parameterized observations, $obs_{Par.}$, explained in chapter 3. The variable p, with $p>0$, defines on the one hand the degree of the single basis function and on the other hand the number of linear combined basis functions. The local behavior of the curve is controlled by the distance between the knots. The smaller the spans the more curvature changes / details can be modeled.

Further parameters of the B-Splines are the control points, $CP_{X/Y}$, which can be stated as weights for each basis function $N_{i,p}$

$$C_{X/Y}\left(obs_{Par.}\right)=\sum_{i=0}^{n}N_{i,p}\left(obs_{Par.}\right) * CP_{X/Y,i}\ , \quad (2.5)$$

where $C_{X/Y}$ is the curve point at the 2D Euclidian space (X, Y) with the homologues curve position $obs_{Par.}$ at the parameter space. For clarity reasons we restrict to the 2D case, the extension to the 3D case is a formal analogy. The geometric continuities depends on the span width and can be restricted if necessary.

3. State of the art in B-Spline curve approximation

B-Spline curve approximation from 2D TLS profiles is a new field in engineering geodesy that refers to the deformation analyses, as shown in [6], [7].The characteristic of a TLS point cloud is normally its high point density and its homogeneous distributed points without gaps.

The standard method for the parameterization of the observations from the metrology, $obs_{X/Y}$ (measured 2D coordinates), is denoted as uniform, where the homologous parameters, $obs_{Par.}$, are equal allocated along the curve. However, this is mostly not the case for measured data. A second method based on the chord length between the $obs_{X/Y}$. It roughly approximates the arc length of the curve. A third one is the centripetal method, which contains the centripetal acceleration and curvature. Lee describes in [8] all three methods in detail, compares them to each other and gives recommendations for deploying them, seen in [9].

The control points are estimated by solving the linear system of equations (2.5). The degree of the basis functions is set empirically to a fix value in accordance to the experience about the observations, the further applications and the requirements to the curve continuity.

The last parameters are the knots, which are necessary for the formulation of the basis functions (2.2). There are two estimation issues referring to the knots: their number and their location inside the knot vector. The last is the most complex one. For the number of knots, the Akaike information criterion, AIC, provides promising results, shown in [7], [10] and [11]. Regarding the location of the knots the uniform distribution performs poorly on heavy irregular curved data sets. For this fact other algorithms perform better. They depend on the distribution of the observations, like the basic method described in [5] and its extended version in [12] by considering the Schoenberg-Whitney condition [13]. A further algorithm is the section midpoint strategy, which locates a new knot in the middle of a span, or at the location with the highest residual to an estimated curve. Other techniques uses a initial length and curvature for the knot placement, e. g. [14], [15]. Calculating initial length and curvature on noisy data is a challenge, but produces sufficient knot locations when reliable parameters (curvature and length) can be calculated. Estimating the location of the knots during the approximation leads to a highly nonlinear optimization problem as mentioned before, which is denoted as the "lethargy", extensively explained in [16]. The motivation of optimizing the knot location despite the lethargy is described in the following chapter.

4. Motivation of the knot optimization

Shown in chapter 3, B-Splines consist of two parameter sets which can be estimated during an approximation. Previous research has shown that the estimation of only one parameter set, the control points, in the linear system may lead to systematic effects in the residuals. Increasing the number of knots increases the number of control points with their connectedness of (2.4) and creates significantly better results, e. g. Figure 1 and [7]. Not only the number of knots improve the approximation results but also their location. Its effect is shown exemplary in the following figure.

Figure 1a shows a section of an under determined approximation result created from the sample Dataset of chapter 6.2. Improving the approximation can be done by increasing the number of knots at specific locations, shown in Figure 1b and 1c. Figure 1d, 1e and 1f show the knot locations inside the knot vector for the curves above. Knots with the same value are printed one below the other. The impact of only one additional knot, seen in Figure 1d at location −4.3, results in highly changes of the curvature shape. The reason for the changes is given by the functional relationship between the knots and their basis functions, seen in from (2.2). The additional knot does not only extend the functional system with one basis function it changes the p ascending basis function, counted from the ad-

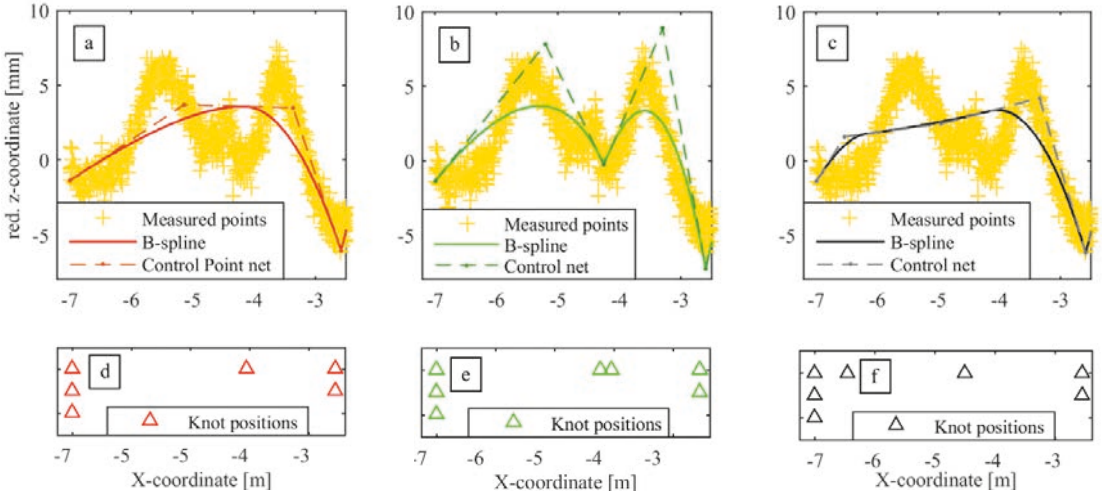

Fig. 1: a) Example of an underdetermined B-Spline approximation; b) Example of an underdetermined B-Spline approximation with one additional knot; c) Example of an underdetermined B-Spline approximation with one additional knot at another location; d) Knot sequence of the curve in a; e) Knot sequence of the curve in b; f) Knot sequence of the curve in c

ditional inserted one. Associated with the knots are the control points, which reinforce or weaken the influence of each basis function, like weights for the observations in a least squares.

The influence of the knot location itself can be seen on the different curves in Figure 1b and 1c. This leads to the fact that the locations of the knots are as important as their number.

5. Implementation

The developed approximation method describes an iterative two-step estimation of the control points and knot locations. For this method, equal observation variances are assumed. The noise assumption ensures that only systematic effects based on the geometry and not on the metrology are optimized and that the numbers of residuals are equally distributed at each span. This is why for now the identity matrix was applied to the stochastic model.

The following flow chart shows the different steps of the method:

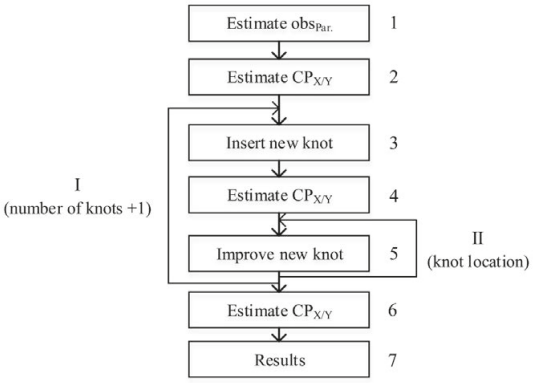

Fig. 2: Algorithm flow chart

In the first step the homologous parameters, $obs_{par.}$, for the measured 2D points, $obs_{X/Y}$, are estimated with one of the methods, uniform or centripetal, appropriated to the datasets as described in chapter 3. In the 2nd step the control points for the minimal configuration of the B-splines, denoted as Bézier curve, with $p+1$ basis functions and a knot vector consisting of

$$U = \{0_0, \ldots .0_p, 1_{p+1}, \ldots ,1_m\}, \qquad (4.1)$$

are estimated using (2.5) in a linear least squares Gauß-Markov model. For the B-Splines used here, the first and last control point fit the first and last observation respectively. These restrictions and the composition of the minimal knot vector implies, that the slope of the line between the first and second control point and between the last and penultimate control point is equal to the slope of the curves at the start and end point. The restrictions are necessary to prevent oscillations of the curve at these points. They are valid for all approximations, which are performed here. If the residuals obtained from the control-point estimation do not fulfil a certain quality criterion, new knots and their locations are estimated iteratively within the loop I (step 3 – 5). In each span cumulative sums (CumSum) of squared residuals are calculated in two versions, first starting from left to right and second starting from right to left. The idea of using the cumulated sums of squared residuals based on equal variances inside each span. Different variance levels indicate systematic effects in the results of the least squares approximation. As shown in chapter 4 the number of knots and their location influences the obtained variance of residuals. Creating a criterion based on the variance, which reduces its value at a specific location inside the approximation, is needed to develop plausible initial values for the knots.

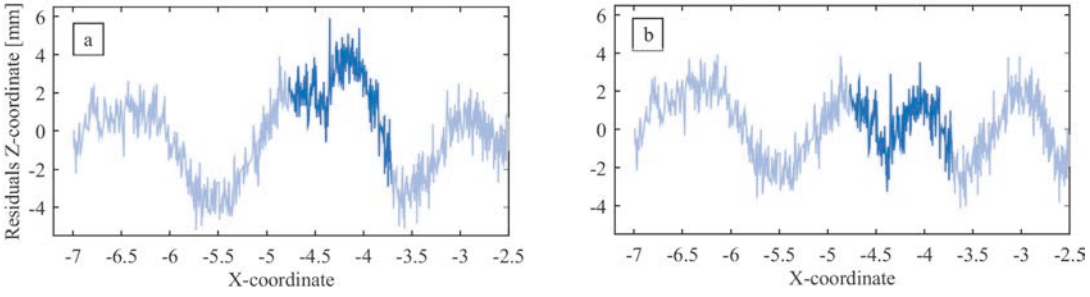

Fig. 3: a) Residuals from approximation shown in Figure 1a; b) Residuals from approximation shown in Figure 1b

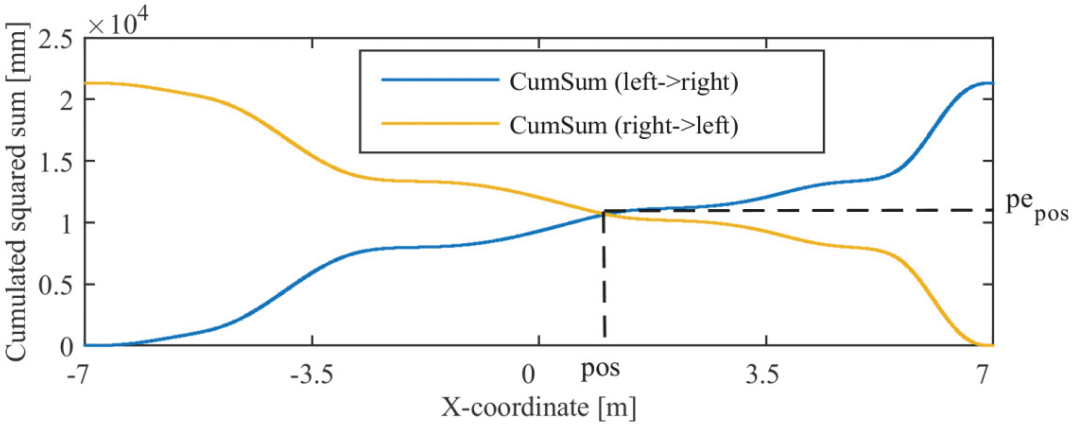

Fig. 4: Cumulated sum of squared residuals (measured data) and their criteria for the new knot locations

These effects can be seen in the residuals, shown in Figure 3, where the additional knot is inserted in the area of –3.7 to –4.7, see Figure 1a and 1b, which corresponds to the section with the highest variance, in this part of the curve. The residuals are reduced by more than the half from ≈5 mm to ≈2 mm at the section mentioned before.

Regarding this concept the squared sum can be understood as the potential energy pe of the residuals inside a span. The position, pos, inside a span where the value of the pe's for both versions of the cumulated squared sum (from left and from right) are equal is defined as the new knot location. Thus, a possible location for a new knot is set equal to the pos in order to reduce the overall pe. At each possible location the value of the cumulative sum at this point is denoted as pe_{pos}, e. g. Figure 4. The new knot will be inserted in the span with the highest pe_{pos} value to reduce the highest pe in the curve.

In each iteration step, only one new knot is inserted. In step 4 the location of the new control points which occurs due to the new knot insertion are estimated with the model (2.5). Afterwards only the location of the new knot is improved by a nonlinear iterative estimation (loop II) using a restricted linearized Gauß-Markov model (step 5). Therefore the location of the new knot is unrestricted while all other knots are fixed by constraints. The Jacobian matrix for this system has the following structure:

$$A = \begin{pmatrix} \frac{\partial C_X\left(obs_{Par.,i}\right)}{\partial u_{p+1}} & \cdots & \frac{\partial C_X\left(obs_{Par.,i}\right)}{\partial u_n} \\ \frac{\partial C_Y\left(obs_{Par.,i}\right)}{\partial u_{p+1}} & \cdots & \frac{\partial C_Y\left(obs_{Par.,i}\right)}{\partial u_n} \\ \vdots & \ddots & \vdots \\ \frac{\partial C_X\left(obs_{Par.,j}\right)}{\partial u_{p+1}} & \cdots & \frac{\partial C_X\left(obs_{Par.,j}\right)}{\partial u_n} \\ \frac{\partial C_Y\left(obs_{Par.,j}\right)}{\partial u_{p+1}} & \cdots & \frac{\partial C_Y\left(obs_{Par.,j}\right)}{\partial u_n} \end{pmatrix}, \quad (4.2)$$

$i = 0, \ldots, j$, $j =$ number of $obs_{par.}$

The derivative for each knot is defined with the recursive algorithms for the basis functions given in (2.2). The parameterization of the observations implies that the $obs_{X/Y}$ provides the full coordinates, here X and Y for the rows, likewise the control points. Due to the orthogonality of the coordinate axes the derivatives of the basis function are the same for each axis.

After the iteration of loop I and II has reached the convergent criterion, based on the results with the simulated data, described later on, the control points are estimated using the optimized new knot location. Then the quality parameters of the results are obtained in step 7. A simultaneous global optimization of the curve parameters, the control points and the knot locations cannot be realized yet due to reasons shown in the next chapter.

Type	Values
Knot vector	{0, 0, 0, 0.10, 0.15, 0.30, 0.55, 0.60, 0.75, 0.90, 1, 1, 1}
Number of knots	13
Number of basis functions / $CP_{X/Y}$	10
Degree	2
Dimension	2 (X,Y)
Noise – Variance	0.005^2
Number of sample points	5000

Tab. 1: B-Spline parameters for simulated data

Method	$\sigma_{apost.}$	T_F	T_F	$F_{9984, 9984, 0.05}$
New method – nonlinear	0.11		1.09	1.03
New method – linear	0.12	1.53		
Basic	0.18			

Tab. 2: Results compared to each other – on simulated data (TF = Test value for the F-test, $F_{f1, f2, 1\text{-}alpha}$ = quantil of the F-distribution)

6. Data Approximation

6.1 Simulated Data

The simulation studies performed in this chapter aim to validate the developed method and to infer its behavior with respect to the knots and control points. Therefore, the test dataset was generated referring to the TLS profile analyzed in chapter 5.2. The noise is processed from the normal distribution with $N(0,\sigma^2 = 0.005^2)$ and used in all simulated data sets. The minimum of 5000 sample points are necessary, because with this number the value σ_{apost}, obtained from the linear approximation in step 2 where the control points are the only unknown, is equal to the value $\sigma_{apriori}$, e. g. Table 1. The sample points are distributed uniformly with a point to point distance of 0.015. The threshold ε to the break criterion of the loop II is set to $\varepsilon = 1e^{-4}$. This value results from the maximum update value for the unknowns of the nonlinear knot estimation in loop II, with the initial values of the control points and knots. The idea is to have the knots and control points as the only unknowns and take the other parameters from the simulated dataset, so that the only influence of changes in the curve geometry relies on them.

Different estimation scenarios were applied on the simulated curve:

- The new method – nonlinear (including loop II, with optimization of knot location in restricted Gauß-Markov model),
- The new method – linear (without loop II, knot location defined according to Figure 4),
- The basic/state of the art method.

also described in Table 2. The degree of the basis function and the number of knots were set equal to the ones of the designed B-Spline. All three above-mentioned methods of parameterization were applied to the $obs_{X/Y}$. A comparison of the obtained results is given in Table 3. For further processing the $obs_{Par.}$ were not improved or recalculated. Instead, they were taken directly from the designed B-Spline.

Results

The Schoenberg-Whitney conditions are fulfilled otherwise the functional matrix of the Gauß-Markov model is singular, which is difficult to solve without further information such as constraints. The linearized normal equation system is badly scaled and needs to be preconditioned to avoid numerical instabilities and to minimize the number of iterations.

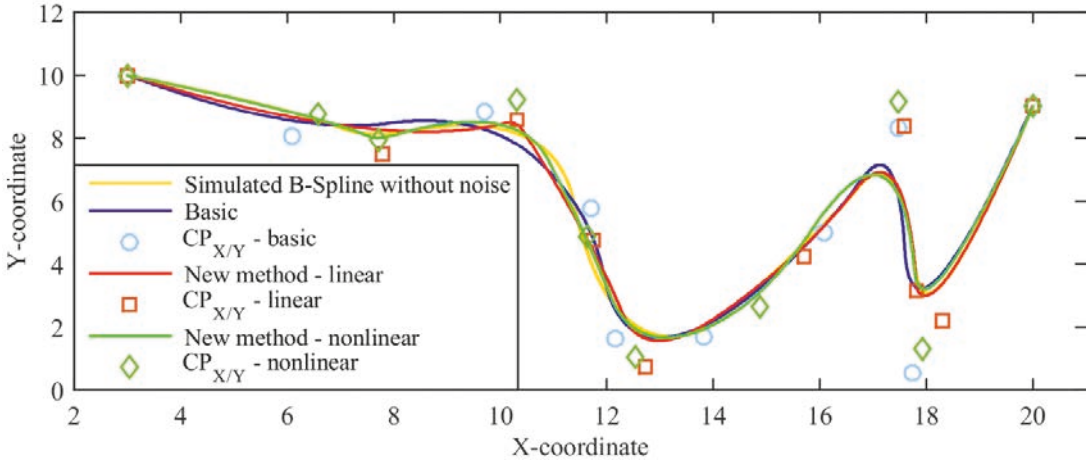

Fig. 5: Result of the B-Spline curve approximations – simulated data

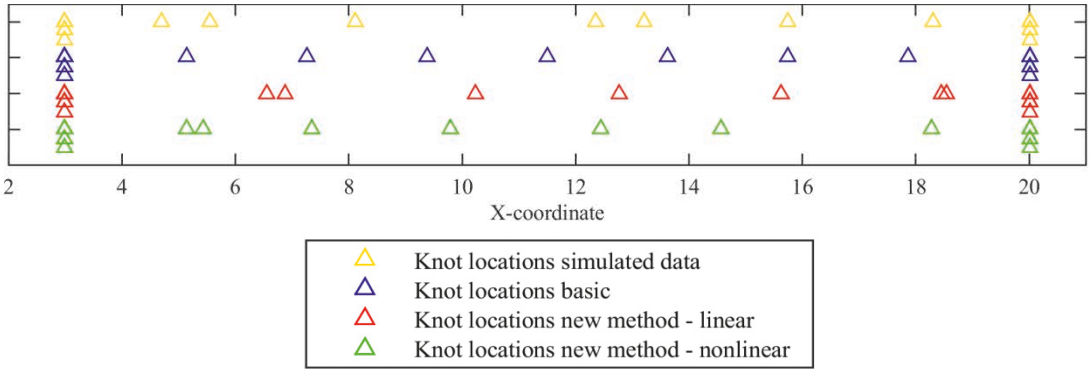

Fig. 6: Knot locations – simulated data

Both new methods show "significantly" better results than the basic one, in case of uncorrelated variances. The connected lines at the columns T_F in Table 2, Table 3 and Table 5 reveal both methods which are compared in the hypothesis test. For example the test value T_F between the basic and the new method linear and between the new method linear and nonlinear respectively is higher than its quantil. The obtained curves are shown in Figure 5.

The highest residuals are at the beginning where the new method produces sharp peaks in the linear case. The reason for that are the short spans at some locations in the knot vector. The new nonlinear method is closer to the $obs_{X/Y}$, but with a high curvature turn and smoother than the linear method. The basic method leads to a shift at the beginning of the curve up to $X \approx 11$ compared to the simulated dataset, which can be interpreted with a shift of the knots at that part. No systematic effects can be observed from the distribution of the control points.

Figure 6 shows the location of the knots for all used B-Splines. The locations of all knots differ from the simulated ones. Instead to the new method – nonlinear, which tend to have a similar knot location pattern as the simulated data. Although there is a significant improvement of the results, most knot locations of the simulated data cannot be reached.

Hypothesis tests cannot be performed correctly on the results, because in our case the

Noise	Parameterization method	$s_{apost.}$	T_F	T_F	$F_{9984, 9984, 0.05}$
Yes	Chordal	0.2932		56	1.034
Yes	Uniform (simulated)	0.0052	40		
Yes	Centripetal	0.2120			

Tab. 3: Results of linear least squares with different obs values (TF = Test value for the F-test, $F_{f1, f2, 1-alpha}$ = quantil of the F-distribution)

Type	Values
Number of knots	22
Number of basis functions / $CP_{X/Y}$	19
Degree	2
Dimension	2 (Z, X)
Sample points	5000 / 12293

Tab. 4: Parameters for the B-Spline approximation of the measured data

Num. Points	Method	$s_{apost.}$ [mm]	T_F	T_F	$F_{9940, 9940, 0.05}$ / $F_{24526, 24526, 0.05}$
5000	New method nonlinear	0.68		1.07	1.03
	New method linear	0.73	1.33		
	Basic	0.97			
12293	New method nonlinear	0.70		1.07	1.02
	New method linear	0.75	1.25		
	Basic	0.94			

Tab. 5: Results compared to each other – on measured data (TF = Test value for the F-test, $F_{f1, f2, 1-alpha}$ = quantil of the F-distribution)

functional model of each method changes. The reason is the different knot vector, which affects the calculated basis functions and the affiliation of the $obs_{Par.}$ to the basis functions. This aspect justifies the sequential knot optimization: the updates of the knot location in loop II are related to the actual functional model and not to the new one that accounts for changes of the basis-function-allocation and the relation of the $obs_{Par.}$ to the basis-functions. Different experiments on the dataset have shown that by estimating all knots at the same time the function changes increase so much, that the nonlinear model fails after the third iteration.

The reason for using the parameters of the simulated B-Spline itself is given by the differences between the three mentioned methods. The parameters differ significantly in the part of the curve with high curvature. As a result of this all known parameterization methods allocate insufficient $obs_{Par.}$ between the spans for the further approximation algorithms. This can be noticed in Table 3, where all linear approximations of the control points differ significantly from the ones obtained for the uniform case.

6.2 Measured Data

The measured data comes from a TLS profile scan, with a total length of 14m. The Z coordinate needs to be sensitive. Therefore it is trend reduced and scaled to [mm]. The X-coordinate is in [m] and represents the step size of points. The point density was reduced from 12293 to 5000

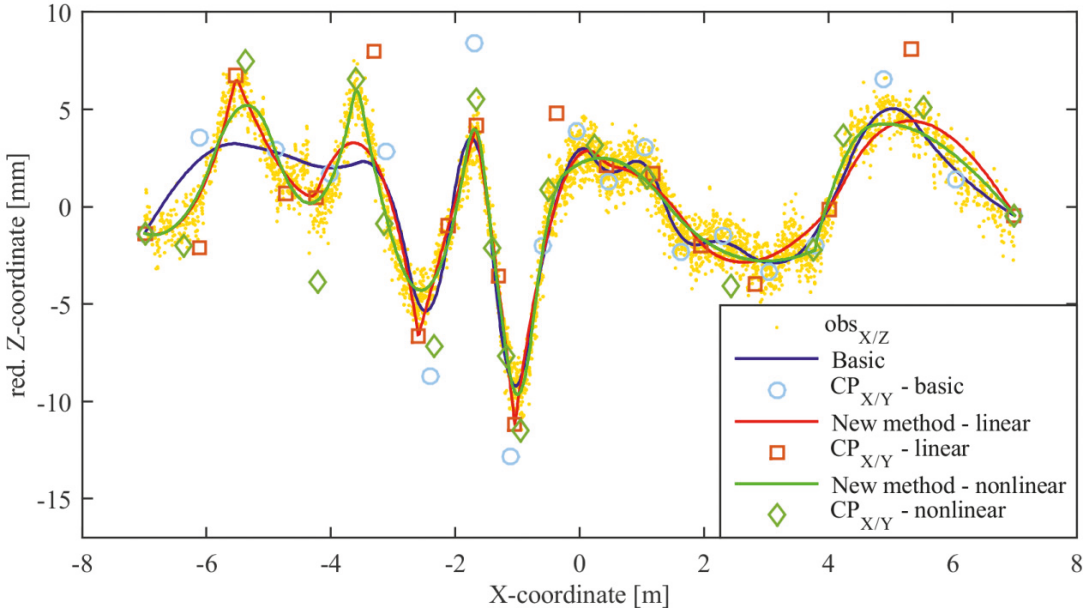

Fig. 7: Result of the B-Spline curve approximation – measured data

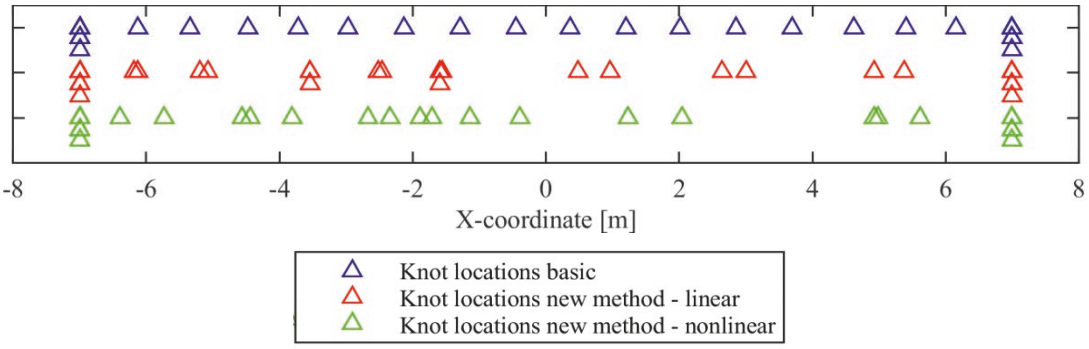

Fig. 8: Knot locations – measured data

points in order to emphasize the impact of the step size. The parameters for the B-Splines are given in Table 4.

The curve parameters allocated to the $obs_{X/Y}$ are calculated with the centripetal method. It has generated the best result compared to the other parameterization methods.

Results

The estimation results are summarized in Table 5. As can be seen the new methods are better than the basic one. However, the decrease of the standard deviation of the control-point estimation is not as strong as in the case of the simulated data set. The variation of the number of knots, degree of the basis function and the number of $obs_{X/Y}$ results in the gradation from the best result by the new method nonlinear to the basic method, as in Table 5. The "significant" changes need to be carefully interpreted with the difficulties of the hypotheses test in mind, mention in chapter 6.1. More explanation of how to read the table can be achieved under Table 2.

Figure 7 shows the different B-Spline curves after the knot estimation with the three methods in the case of 5000 sample points.

Especially at the beginning of the curve, the new methods lead to improved approximations

of $obs_{X/Y}$. In the section between 0 m and 4 m the approximation with the basic method is more detailed. These oscillations appear also in the case of estimation with the developed methods when a higher number of knots are used. The difference between the linear and the nonlinear case of the developed method is the smoothness of the curve. While in the linear case the curve is approximated with sharp peaks the nonlinear model leads to rounded peaks and a smoother curve.

Figure 8 shows the knot distribution in the knot vector. Noticeable are the large differences of the knot locations between the methods, which can also be seen in Figure 6. The reason for that are the large functional changes in the formulas between different parameter sets, which produce large differences in the residuals on which the new parameters rely on.

7. Conclusion

The new methods for the knot estimation improve the approximation of TLS profiles with B-Splines. The algorithms were validated with simulated data and applied on real data. They lead to better results than the basic method.

Despite the functional problems during the nonlinear iteration the algorithm converges when estimating only one knot at a time and allowing only small updates. This leads to good results also in case of higher knot numbers. The method doesn't use any problem specific smoothing or penalty terms. When estimating all knot locations at once the algorithm becomes unstable. Oscillations like in the case of polynomials with higher degree didn't occur when the estimation was performed by a maximum of 23 knots in order to reach the standard deviation of the simulated dataset.

Different parameterizations of the observations were implemented in order to analyze their influence on the approximation results. This influence tends to be higher than the influence of the right number of the knots. Similar approximation results were obtained for different numbers of $obs_{X/Y}$.

Extending the sequential nonlinear model to a global estimation of knots and control points is aimed in future research.

References

[1] Workshop Flächenrepräsentation. Workshop at the DGK Sektion Ingenieurgeodäsie, Rhön-Park, 2013.

[2] C. Schmitt, H. Neuner, I. Neumann, J. Piehler, M. Hansen, and S. Marx, Erstellung von Ist-Geometrien für strukturmechanische Berechnungen. Beiträge zum 17. Internationalen Ingenieurvermessungskurs Zürich, A. Wieser, Ed. Heidelberg, Wichmann Verlag, 2014, 37–48.

[3] C. de Boor, A practical guide to splines. New York; Berlin [u.a.], Springer, 1978.

[4] P. de Casteljau, Courbes et surfaces a pôles. André Citron Automobiles SA - Paris, 1959.

[5] C. Schmitt, H. Neuner, and I. Neumann, Strain detection on bridge constructions with kinematic laser scanning. Proceedings of the 2nd Joint international Symposium on Deformation Monitoring, 2013.

[6] H. Neuner, C. Schmitt, and I. Neumann, Modelling of terrestrial laser-scanning profile measurements with B-Splines. Proceedings of the 2nd Joint international Symposium on Deformation Monitoring, 2013.

[7] E. T. Y. Lee, Choosing nodes in parametric curve interpolation. Comput.-Aided Des., 1989, 21, 6, 363–370.

[8] P. Dierckx, Curve and surface fitting with splines. Oxford, Clarendon Press, 1995.

[9] M. J. Lindstrom, Penalized Estimation of Free-Knot Splines. J. Comput. Graph. Stat., Jun. 1999, 8, 2, 333–352.

[10] C. Harmening and H. Neuner, Raumkontinuierliche Modellierung mit Freiformflächen. Terrestrisches Laserscanning 2014 (TLS 2014) | Beiträge zum 139. DVW-Seminar, 1st ed., 78, Fulda, 2014, 228.

[11] L. A. Piegl and W. Tiller, The Nurbs Book. Springer, 1997.

[12] L. A. Piegl and W. Tiller, Surface approximation to scanned data. Vis. Comput., Nov. 2000, 16, 7, 386–395.

[13] I. J. Schoenberg and A. Whitney, On Polya Frequency Function. III. The Positivity of Translation Determinants With an Application to the Interpolation Problem by Spline Curves. Trans. Am. Math. Soc., 1953, 74, 2, pp. 246–259.

[14] A. Razdan, Knot Placement for B-Spline Curve Approximation. 1999.

[15] H. Park and J.-H. Lee, B-spline curve fitting based on adaptive curve refinement using dominant points. Comput.-Aided Des., Jun. 2007, 39, 6, 439–451.

[16] D. L. B. Jupp, The "Lethargy" theorem—A property of approximation by γ-polynomials. J. Approx. Theory, Jul. 1975, 14, 3, 204–217.

Contacts

Univ.-Ass. MSc. Claudius Schmitt, Vienna University of Technology, Department of Geodesy and Geoinformation, Engineering Geodesy, Gusshausstraße 27-29, E120-5, 1040 Vienna, Austria.

E-Mail: claudius.schmitt@geo.tuwien.ac.at

Prof. Dr.-Ing. Hans Neuner, Vienna University of Technology, Department of Geodesy and Geoinformation, Engineering Geodesy, Gusshausstraße 27-29, E120-5, 1040 Vienna, Austria.

E-Mail: hans.neuner@geo.tuwien.ac.at